SLAC-TN-15-033

Channeling, Volume Reflection and Gamma Emission Using 14GeV Electrons in Bent Silicon Crystals

B. Benson

(Dated: 14 August 2015)

High energy electrons can be deflected with very tight bending radius using a bent silicon crystal. This produces gamma radiation. As these crystals can be thin, a series of bent silicon crystals with alternating direction has the potential to produce coherent gamma radiation with reasonable energy of the driving electron beam. Such an electron crystal undulator offers the prospect for higher energy radiation at lower cost than current methods. Permanent magnetic undulators like LCLS at SLAC National Accelerator Laboratory are expensive and very large (about 100 m in case of the LCLS undulator). Silicon crystals are inexpensive and compact when compared to the large magnetic undulators. Additionally, such a high energy coherent light source could be used for probing through materials currently impenetrable by x-rays. In this work we present the experimental data and analysis of experiment T523 conducted at SLAC National Accelerator Laboratory. We collected the spectrum of gamma ray emission from 14 GeV electrons on a bent silicon crystal counting single photons. We also investigated the dynamics of electron motion in the crystal i.e. processes of channeling and volume reflection at 14 GeV, extending and building off previous work. Our single photon spectrum for the amorphous crystal orientation is consistent with bremsstrahlung radiation and the volume reflection crystal orientation shows a trend consistent with synchrotron radiation at a critical energy of 740 MeV. We observe that in these two cases the data are consistent, but we make no further claims because of statistical limitations. We also extended the known energy range of electron crystal dechanneling length and channeling efficiency to 14 GeV.

I. INTRODUCTION

Accelerator undulators are used to create coherent light. At SLAC, LCLS produces the brightest X-ray beams in the world, allowing researchers to probe deep enough to track chemical reactions and create videos on the atomic level. Undulators responsible for this light, however, face certain limitations. Magnetic undulators like the ones at LCLS are very large and very expensive. There is therefore room for improvement with new technology. A candidate for this new technology is the use of high energy electrons deflected by bent crystals.

Electrons deflected by a series of bent crystals could zigzag, mimicking the undulation induced by powerful magnets. This electron motion can be possible with the use of crystals, resulting in coherent gamma radiation. But the dynamics of electrons in crystals and the spectrum of radiation produced must be well understood before undulators of this nature can be attempted. Crystals are used in accelerator physics to direct charged particles. Most often, however, bent crystals are used to extract protons from the beam. Upon channeling, protons tend to pass in between the atomic planes thus having a reduced probability of scattering off the nuclei. Therefore they channel well over comparatively long distances. Electrons, being attracted by the nuclei tend to have an increased probability of scattering off nuclei and therefore they channel only over very short distances (10s of μm). As a result, the dynamics of protons in bent crystals are reasonably well understood. There is much less known about the dynamics of electrons in bent crystals.

In order to better understand the dynamics of electrons in bent crystals, previous work[1] has measured parameters such as dechanneling length, channeling efficiency, and volume reflection angle at energies of 3 to 6 GeV. And subsequent unpublished work[2] has extended these measurements up to 10 GeV. Their work includes the three key crystal orientations for the production of gamma radiation: amorphous, channeling, and volume reflection. After understanding the electron dynamics within bent crystals in each of these orientations, it is important to understand the radiation produced by the electron motion. Only very little data for gamma-ray spectra has been published.

In this paper, we extend the work described in[1] and[2] by measuring dechanneling length, channeling efficiency, and volume reflection angle at 14 GeV. We also present measurements of the resulting gamma radiation spectrum in each of the three crystal orientations.

II. EXPERIMENTAL SET-UP AND PROCEDURE

In this experiment have two main objectives: to detect electron dynamics and gamma radiation. Thus, set-up, procedure, and analysis, are presented for both electron dynamics and gamma radiation

A. Set-Up: Electron Dynamics

The silicon (Si) crystal used in this experiment was fabricated at the Sensors and Semiconductor Laboratory at the University of Ferrara with crystallographic orientation chosen to produce quasi-mosaic bending of the (111) plane. Its thickness was measured interferometrically to be 60± 1 mum. The (111) plane has a bending

SLAC National Accelerator Laboratory, 2575 Sand Hill Road, Menlo Park, CA 94025

This material is based upon work supported by the U.S. Department of Energy, Office of Science, Office of Workforce Development for Teachers and Scientists (WDTS) under the Science Undergraduate Laboratory Internship (SULI) program, under Contract No. DE-AC02-76SF00515.

FIG. 1. crystal stage inside the scattering chamber (beam enters from the top of the figure)

radius of 0.15 m giving a total bending angle of the crystal of $\theta = 402 \pm 9\mu$rad in the horizontal direction. The crystal was mounted in a scattering chamber in the End station A Test Beam. A rotational stage allows rotation of the crystal with step sizes of roughly 10 μrad. A translational stage allows moving the crystal into the beam and selecting the optimal position. A flat mirror mounted on the side of the crystal holder reflecting a laser beam to a screen at a distance of about 1 m provides a measurement of the crystal rotation angle with a resolution below 5 μrad. The crystal stage and the scattering chamber can be seen from the top down in Figure 1. A Cerium doped Yttrium Aluminum Garnet (YAG) screen of 500μm thickness with a CCD camera 13 m down stream of the crystal provides the means of data acquisition in this experiment. The YAG screen is pitched by 45 degrees towards the camera. The camera is linear and saturates hard at 255. We adjusted the gain on the camera to avoid this.

B. Procedure: Electron Dynamics

a. Calibration. For pixel calibration, a circle was fitted along the edge of the screen. This circle had a radius of 2131 pixels, and the radius of the YAG screen is 10 mm. This was used along with the distance from the crystal to the YAG screen to calibrate the camera, finding 213 pixels/mm and .36 μ Rad/pixel. Over the course of 24 hours, we found that the laser we used to calibrate crystal angle would drift. This drifting of the laser caused error in crystal orientation during later runs. We expect that collecting data for this part of the experiment was not affected by this because it took only 1 to 2 hours.

b. Data Collection. Experimental measurements were performed by rotating the crystal in small angular steps and recording an image of the circular YAG screen.

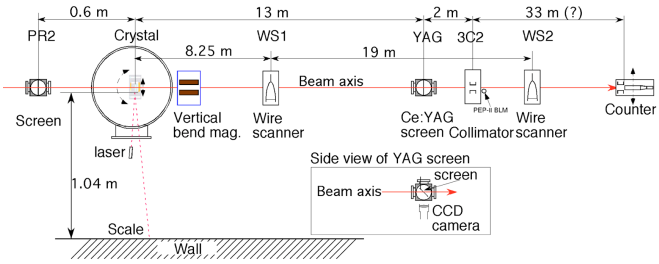

FIG. 2. beam line set-up for detecting electron dynamics and radiation

We moved the crystal horizontally until the beam intersected the crystal near its vertical edge. This is the location where we believe the crystal has the most constant radius of curvature. A region of the screen is chosen to avoid the edge of the YAG screen and to include the full extent of the beam spot. We extract a horizontal intensity profile by removing a 2.3 degree rotation and integrating vertically. We then normalize to 1 to obtain a probability distribution. Probability distributions taken at the same crystal angle are combined by shifting each such that it has an expectation value equal to the mean of the groups expectation values. The resulting plots are then averaged so that each crystal angle corresponds to one probability distribution. By plotting these distribution along the y-axis for each crystal angle along the x-axis one obtains the so called triangle plots.

C. Set-Up: Gamma Spectrum

We inserted a vertical bending magnet after the crystal scattering chamber and a copper collimator with diameter 16.7μm, 15 m downstream of the crystal. The vertical bending magnet deflects electrons into this collimator (3C2), allowing only uncharged particles i.e. photons through the collimator. A photo multiplier tube (PMT for short) placed about 50 m downstream of the crystal was the main diagnostic detecting the radiation produced by the crystal in the beam. Lead bricks were placed in front of the PMT, allowing only a 3 mm vertical collimated slit of radiation to enter. The whole ensemble was placed on a moving platform, allowing controlled scanning in the horizontal direction, while integrating over vertical radiation. The set-up can be seen in Figure 2.

D. Procedure: Electron Gamma Spectrum

c. Calibration. A primary beam of bunch charge 1E9 and energy 14.74 GeV was used to calibrate the horizontal location of the PMT. After turning the vertical bending magnet on and deflecting the particles into the collimator, the PMT was scanned across horizontal positions in increments of 2.5mm. At each position PMT recorded intensity for about 1000 triggers different The

PMT recorded intensity as it was scanned horizontally in increments of 2.5mm. This was done without the crystal in the beam (called background), and with the crystal in each orientation: amorphous, channeling, and volume reflection. At each position in the PMT scan, we average over the 1000 triggers and plot position vs energy. We compare each of the three crystal orientations with the background scan, in an effort to find the PMT position that maximizes the crystal signal over the background signal. We measure position of the PMT in mm; only relative position to the center of the beam matters. For the amorphous orientation we chose 340 mm as the location of the detector, for channeling we chose 335 mm, and for volume reflection we chose 345 mm. We picked these detector locations after a preliminary scan of the PMT using horizontal increments of 5mm. Later, we performed a scan on all crystal orientations and background using horizontal increments of 2.5mm. After analyzing the more finely spaced data, we realized that these positions we chose do not result in maximum signal to noise intensity. In the future, we will analyze this further and make a more careful selection of PMT position.

We also used the primary beam to set crystal orientation. For channeling, we rotated the crystal in small angular steps recording the angle of maximum channeling intensity. Similarly, we chose an angle for volume reflection orientation such that we could tolerate large beam jitter and while staying in the volume reflection orientation. For the amorphous orientation we chose an angle far from channeling, so that our calibration was robust against beam jitter. Our recorded angles of these crystal orientations are prone to error due to the slow drifting of our angle calibration laser.

The single-electron beam was prepared by inserting a thick Cu target in the beam line and collimated the beam in energy and size using SL10 and 24C collimators.

The single electron energy was used to calibrate the gain of the PMT. Starting with 1550 volts across the PMT, we reduced the beam until we could see the 1 electron, 2 electron, and 3 electron peaks on the PMT. The PMT is assumed to be linear and each trigger is recorded as a charge between 0 and 400, pc. We increased the voltage on the PMT from 1550 to 1650 in increments of 25, recording how the single electron peak rose towards 400 on the PMT. PMT gain is known to be exponential in voltage. We, therefore, use PMT Q= $A * e^{b*V}$ as a fit for our five points. We then chose a voltage of 1775 volts to take our spectra. The beam had an energy of 13.97 GeV, so this would put the single electron peak of 13.97 GeV above PMT channel number 1000. This results in a window from PMT channel number 0 to 400 of about 0 to 5 GeV.

We opened collimator SL10 and 24C until we had 5 to 6 electrons in our beam. We expect approximately .03 photons per electron, thus within reasonable error, this beam should result in emission of single photons.

d. Data Collection. For a given crystal orientation, we set the PMT to its respective position, we inserted the crystal at the calibrated angle orientation, and we turned on the vertical bending magnet. We then collected 5 pulses/sec until we had about 18000 triggers on the PMT. We did this 6 times, one without the crystal and one with the crystal for each of the 3 orientations.

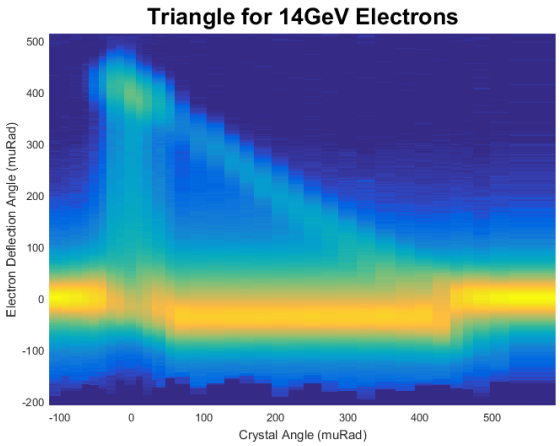

FIG. 3. Final triangle plot with 14 GeV electrons after jitter reduction

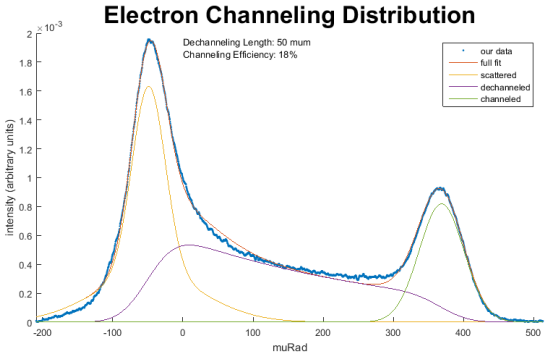

FIG. 4. dechanneling fit used to extract dechanneling length and channeling efficiency

III. ANALYSIS

A. Analysis: Electron Dynamics

While taking data during the experiment, the beam was unstable and contained a lot of jitter. When constructing the triangle plot, became clear that this jitter was too large to create a smooth triangle plot. In order to reduce this jitter, vertical slices had to be shifted up or down to match with their neighbors. The relative movement of these slices increases the quality of the picture. We believe that this does not reduce the amount of information within the plots, although, this requires further discussion.

We began by breaking the triangle plot into 4 sections

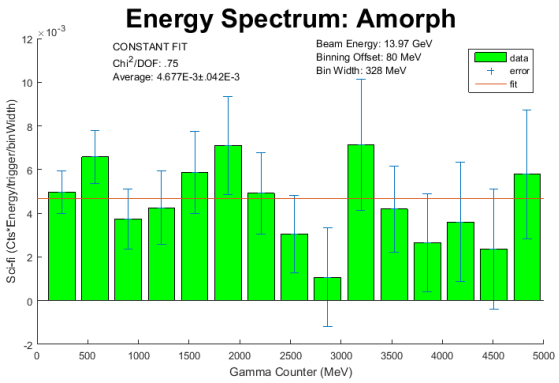

FIG. 5. Single photon energy spectrum: Amorphous crystal orientation

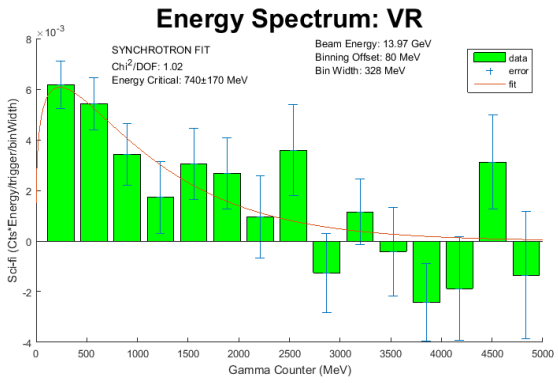

FIG. 6. Single photon energy spectrum: Volume Reflection crystal orientation

based on crystal orientation. These sections in order are amorphous one, channeling, volume reflection, and amorphous two. For the amorphous and volume reflection sections, we found the peak of each slice and aligned this peak with the average of all amorphous peaks and volume reflection peaks respectively. For the channeling section, we had two steps. The first step involves aligning the first channeling slice with its amorphous neighbor and then shifting the following slices vertically until they are most strongly correlated with their neighboring slice to the left. The next step is to introduce a constant slope between slices by shifting each slice down by a constant relative to its left neighbor. We pick this slope such that it results in the final channeling slice aligning with the first volume reflection slice. After this, the slice between channeling and volume reflection and the slice between volume reflection and amorphous two were shifted vertically by hand to make the transitions between sections look smoother.

After doing this, it is clear that neighboring slices within the plot have very similar shape. This is consistent with our initial assumption that beam jitter is mostly spacial. The triangle plot can be seen in log scale in Figure 3.

After obtaining the channeling probability distribution, we followed the procedure outlined in[2] to extract the channeling parameters. This includes determining two parameters defined by Wistisen et al. by using the amorphous distribution: A and r. They define the shape of the peaks in the distributions. We found these parameters using 6 YAG screen shots i.e. the first and last three YAG screens. For each of the 6, we calculated A and r. We then averaged the 6 values to get the final values of A and r. We then used these parameters in the remainder of the fitting procedure, seen in Figure 4

B. Analysis: Electron Gamma Spectrum

We chose to bin with bin width of 333MeV, we then normalize our histogram by triggers and binwidth. We

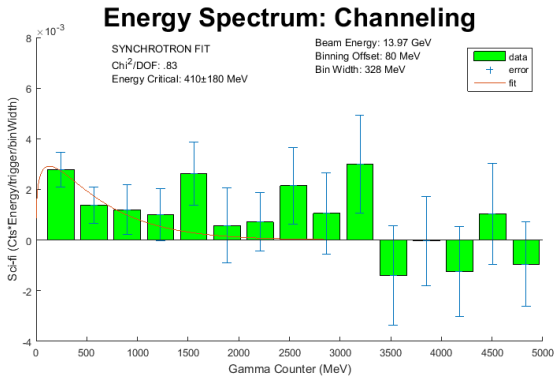

FIG. 7. Single photon energy spectrum: Channeling crystal orientation

define 1 sigma of error for each bin as $\sqrt{N}$ where N is the number of triggers in that bin. In all 6 cases, the first bin contains a majority of the triggers in the histogram. After subtracting the background spectrum from the corresponding crystal spectrum, error adds in quadrature. The first bin in the histogram then has an error that is much too large. To avoid this, we choose an energy threshold such that everything below this energy is counted as zero. We use Figure 8 to find this threshold. For a given threshold, we define HitRate as the number of triggers above the threshold divided by the total number of triggers. HitRate with the crystal in over HitRate with the crystal out of the beam gives us a measure of signal to noise. Essentially, we plot threshold versus this signal to noise ratio. Above the correct threshold, we expect signal to noise to be approximately constant. In Figure 8 we see a clear change in signal to noise between 80 and 90 MeV for all crystal orientations. In the figure we call the x-axis 'MeV Offset'. This is the same as the threshold already discussed. After averaging each of the curves in this plot, we see that 80 MeV Offset looks closer to the true value. Thus we set our threshold at 80 MeV.

We also note that all crystal orientation result in single photon energy spectra that look approximately like

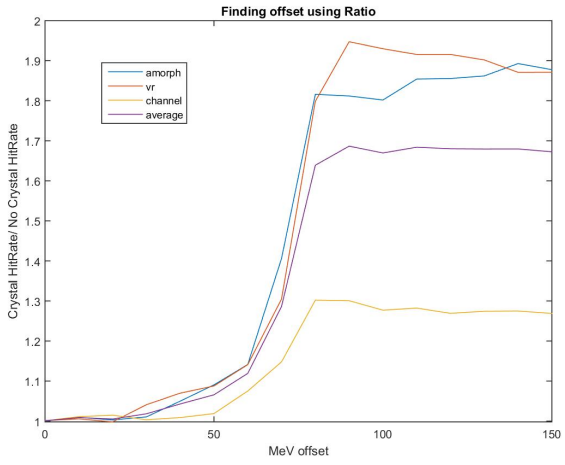

FIG. 8. determining threshold using signal to noise

$\frac{1}{Energy}$. In the case of bremsstrahlung, this dependence is exactly $\frac{1}{Energy}$. Thus, we cancel this dependence by weighting each of our bin counts by the Energy of that bin. This allows for better comparison of spectra.

IV. RESULTS AND DISCUSSION

Figure 3 shows the triangle after jitter reduction. In this figure, we find the Volume Reflection Angle by calculating the average deflection angle of the main beam in volume reflection. We also show the fit for the dechanneling probability distribution in Figure 4. This fit was used to calculate Dechanneling Length and Channeling Efficiency. The following are the values for all electron dynamic parameters during this experiment that can be compared to parameters used in[2]:

A	3.25
r	.55
Dechanneling Length	50 μm
Channeling Efficiency	.18
Volume Reflection Angle	36 μrad

These parameter can be compared to parameters found at lower energies.[21] This comparison will be left for future work.

The quality of fit is only fair. This can be seen in the left tail where the scattered electrons do not match the distribution predicted by A and r. We can also see a discrepancy at the dechanneling slope. One possible explanation could be that a non-negligible amount of electrons rechannel, extending the dechanneling slope. We will explore the fitting procedure in the future to achieve a better fit.

The following figures display the background-subtracted radiation spectra (Figure 5)(Figure 6)(Figure 7). These figures contain the spectra as well as specific fits. For volume reflection and channeling radiation spectra, a synchrotron radiation fit was chosen. For the amorphous radiation spectrum, bremsstrahlung was chosen. In the volume reflection case, we get a good fit and a chi^2 around 1. In the Amorphous case, we also get a good fit and a chi^2 below 1. The channeling fit is not good, however, and error bars are so large that almost any model would work. Thus, we make no further conclusions about the channeling data. Volume reflection and amorphous cases give us trends that our consistent with our expectations.

Volume reflection fits to a synchrotron radiation spectrum consistent with a critical energy of 740 MeV as seen in Figure 6. This corresponds to a bending radius of 8 μm. This is to be compared to the 400 μm bending of channeling. If we take this synchrotron radiation model, the bending radius of electrons in volume reflection is smaller than that of channeling as expected.

V. CONCLUSION

We have defined parameters that extend our knowledge of electron dynamics within crystals from 3 GeV to 14 GeV. We have also seen trends in gamma spectra that are consistent with bremsstrahlung and synchrotron radiation. In future work on electron dynamics, we aim to fit energy dependent formulas to known parameters to predict dynamics at higher energies. In future work on gamma spectra, we aim to reduce background noise and collect more triggers to reduce statistical limitation. Once these gamma spectra are well understood for single crystals, we can align a series of alternating crystals and begin to understand the spectrum of radiation produced by an electron crystalline undulator.

VI. ACKNOWLEDGEMENTS

This work was supported by the U.S. Department of Energy through the Suli program.

Thank you to Uli Wienands for mentoring me throughout the summer.

Thank you to Enrique Cuellar for coordinating the Suli program at SLAC.

[1] U. Wienands, T. M. Markiewicz, J. Nelson, R. Noble, J. L. Turner, U. I. Uggerhoj, T. N. Wistisen, E. Bagli, L. Bandiera, G. Germogli, B. Guidi, A. Mazzolari, T. Holtzapple, and M. Miller, "Observation of deflection of a beam of multi-gev electrons by a thin crystal," Phys. Rev. Lett **114** (2015).

[2] T. Wistisen, U.I.UggerHoj, U. Wienands, T. Markiewicz, E. Bagli, A. Mazzolari, R. Holtzapple, and M. Miller, "A study of channleing, volume reflection and volume capture of 3.35 - 10.5 gev electrons in a bent silicon crystal," to be submitted to Phys. Rev. B. (2015).